

Sulfonated Hierarchical ZSM-5 Zeolite Monoliths as Solid Acid Catalyst for Esterification of Oleic Acid

Binhang Zhao, Pan Yang, Nan Zhang, Donald R. Inns, Elena F. Kozhevnikova, Alexandros P. Katsoulidis, Ivan V. Kozhevnikov, Alexander Steiner, Haifei Zhang*

Department of Chemistry, University of Liverpool, Crown Street, Liverpool L69 7ZD, UK

*Email: zhanghf@liverpool.ac.uk

Electronic Supplementary Information (ESI)

Table of contents:

Experiment details: pages S2 – S7

Tables S1 – S3: page S8 – S10

Figs S1 – S14: pages S12 – S24

Reference: page S25

Experiment Details

Chemicals and reagents

NH₄-ZSM-5 zeolite (SiO₂:Al₂O₃ = 23:1) was bought from Thermo Scientific. Oxalic acid (98%), polyvinyl alcohol (PVA, MW 90,000-100,000, 99% hydrolysis), tetraethyl orthosilicate (98%, TEOS), cetyltrimethylammonium ($\geq 98\%$, CTAB), sodium hydroxide ($\geq 98\%$), hydrogen peroxide solution (34.5-36.5%), oleic acid (65%-88%) and phenolphthalein were supplied by Sigma-Aldrich. Diethyl ether ($\geq 99\%$), methanol ($\geq 99\%$), propan-2-ol ($\geq 99.5\%$), toluene ($\geq 99.8\%$), nitric acid (70%), ethyl acetate ($\geq 99.5\%$), (3-mercaptopropyl) trimethoxysilane (95%, 3-MPTMS) and potassium hydroxide (86.5%) were purchased from Fisher Scientific. Ethanol absolute (99.96%) was bought from VWR.

Preparation of NH₄-ZSM-5 monoliths by ice-templating

0.6 g PVA was added in 20 ml deionized water at 90 °C with stirring at 400 rpm until PVA was completely dissolved. Zeolite suspensions were prepared, with concentrations of 15 wt% relative to the mass of water. 20 ml suspension was sonicated for 5 minutes before freezing in liquid nitrogen. Then frozen samples were placed into the freeze-dryer (CoolSafe, Jencons-VWR) for at least 48 hours.

Modification of NH₄-ZSM-5 monoliths

The obtained NH₄-ZSM-5 monolith was immersed into the TEOS sol with different amount of CTAB. The molar ratio is 1(TEOS): 4(H₂O): 0.0044(Oxalic acid): 0.148(CTAB). Different CTAB concentrations were tested throughout the experiment, with concentration of 0 mol/L, 0.5 mol/L and 0.8 mol/L. The TEOS sol was prepared as followed: 55.8 ml TEOS, 18 ml deionized water and 0.1 g oxalic acid were mixed with 400 rpm for 1 hour in room temperature then stored at -20 °C at least one week for the TEOS hydrolysis. 3 g freeze-dried NH₄-ZSM-5 monolith was immersed in 73.8 ml TEOS sol containing 13.45 g of CTAB (0.5 mol/L) for 4 hours at 4°C. The immersed NH₄-ZSM-5 monolith was placed in a funnel and rinsed with isopropanol for 3 minutes to remove any excess TEOS sol from the fabricated monolith. Finally, the sample was heated at 70 °C in vacuum oven 16 h to complete the gelling process.

Calcination

The samples were calcined in furnace in air. The calcining condition: heat at 1 °C/min to 250 °C, holding 1 hour, then heat to 550 °C at 1 °C/min, hold for 5 hours then cooling to the room temperature at 3 °C/min. The polymer (PVA) and surfactant (CTAB) were removed in this procedure. Meanwhile, the NH₄-ZSM-5 zeolite was converted into H-ZSM-5 during the calcination.¹

Preparation of sulfonated hierarchical ZSM-5 zeolite monoliths

To increase the number of silanol groups within the monoliths, 1 g of calcined monoliths underwent treatment in 25 ml 0.3 mol/L HNO₃ solution at 95 °C for 6 hours. This process was conducted in a round-bottom flask equipped with a condenser. The resulting monoliths were subsequently rinsed three times with water and then subjected to overnight drying in a vacuum oven at 70 °C. Some monoliths were intentionally left untreated with HNO₃ to serve as control samples, facilitating the assessment of the influence of HNO₃ influence.

1g of obtained monoliths were then immersed in a solution comprising 0.6 g of 3-MPTMS and 20 ml of toluene solvent. The experiment was conducted with three different mass ratios of monolith to 3-MPTMS: 1:0.2, 1:0.6, and 1:2.5. This mixture was transferred into a round-bottom flask equipped with a condenser, placed in an oil bath, and maintained at 75 °C for 24 hours. Prior to heat in the oil bath, it underwent a 5-minute ultrasonic treatment. After the reaction, the materials underwent three toluene washes to remove any excess 3-MPTMS, followed by drying in a vacuum oven at 70 °C.

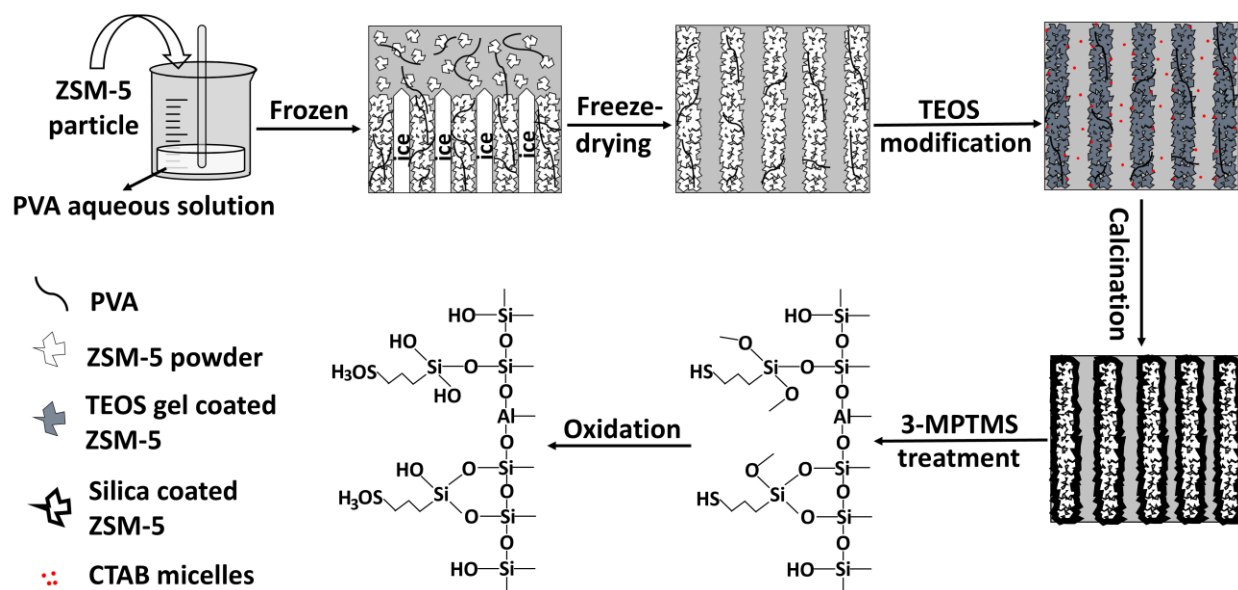
Subsequently, the dried 1g 3-MPTMS-treated monoliths were oxidized with 60 ml of H₂O₂ solution for 24 hours at room temperature. Scheme S1 outlines the complete procedures for fabricating sulfonated hierarchical ZSM-5 monoliths. After oxidation, the monoliths were washed three times with deionized water and then dried in vacuum oven overnight at 70 °C.

The resulting monoliths were denoted as H-A-SO₃-B-Z monoliths, where:

- H indicates treatment with HNO₃,
- A indicates the mass ratio of 3-MPTMS to monoliths,
- B denotes CTAB concentrations,
- Z stands for zeolite.

For instance, 1g monolith with 15 wt% zeolite loading, 0.5 mol/L CTAB in TEOS solution, treated with HNO₃, 0.6 g of 3-MPTMS, and H₂O₂ would be designated as H-(0.6) SO₃-0.5-Z. Monoliths with the same conditions but not treated with HNO₃ would be labelled (0.6) SO₃-0.5-Z. Monoliths under the same conditions but without sulfonation would be denoted as H-0.5-Z. Additionally, some of ZSM-5 particles was directly treated with 3-MPTMS, using a mass ratio of 1:0.6 (ZSM-5 particles to 3-MPTMS),

followed by H₂O₂ treatment. This resulting sample was designated as SO₃-ZSM-5 particles.



Scheme S1. A schematic representation illustrating the production and modification of sulfonated hierarchical ZSM-5 monoliths. Initially, NH₄-ZSM-5 suspensions with PVA are frozen and freeze-dried subsequently to create porous monolith. These freeze-dried monoliths are then treated using TEOS sol with CTAB. The removal of PVA and CTAB through calcination results in hierarchically structured ZSM-5 monoliths. Subsequently, the materials are treated with HNO₃ to introduce more silanol groups and then subjected to 3-MPTMS and H₂O₂ treatments to graft -SO₃ groups, thereby increasing the acid density.

Characterizations

The powder X-ray diffraction (XRD) patterns of zeolite samples were obtained using a Panalytical Empyrean MPD diffractometer, equipped with a high-throughput screening (HTS) XYZ stage, an X-ray focusing mirror and a PIXcel detector. The analysis employed Cu K α radiation over a 2 θ range of 2 to 58°, with a step size of 0.013° in 2 θ and a collection time of 161.3 seconds per step. The morphology of zeolite monoliths was observed by scanning electron microscopy (Hitachi S4800 SEM). A small piece of prepared monolith was adhered to a stub with double-sided carbon tape. The monoliths were then coated with gold using a 15 mA sputter current for 45 s prior to SEM analysis.

N₂ sorption analysis was carried out using a Micrometric 3-Flex 3500 Gas Sorption Analyzer. The zeolite monoliths underwent degassing for 15 h at 100 °C before low-temperature nitrogen adsorption and desorption experiments. The total specific surface area of the sample was measured using the Brunauer-Emmet-Teller (BET) isothermal equation, while the pore size distributions was calculated by the non-

local density functional theory (NLDFT) method. Micropores volume was determined by the T-plot method, and the mesopores volume was assessed using the Barrett–Joyner–Halenda (BJH) method.

X-ray photoelectron spectroscopy (XPS) analysis was performed at the EPSRC National Facility for XPS (“HarwellXPS”), using a Kratos Axis SUPRA XPS equipped with a monochromated Al K α X-ray source 700 \times 300 μ m. High resolution spectra were obtained using a pass energy of 20 eV, step size of 0.1 eV and sweep time of 60 s. Survey spectra were obtained using a pass energy of 160 eV. Charge neutralisation was achieved using an electron flood gun with filament current = 0.38 A, charge balance = 2 V, filament bias = 4.2 V. All data was recorded at a base pressure of below 9×10^{-9} Torr and a room temperature of 294 K. Data was analysed using CasaXPS v2.3.25PR1.0. Spectra were charge corrected to adventitious carbon at 284.8 eV. Peaks were fit with a Shirley background prior to component analysis. Voigt-like functions were used for symmetric line-shapes (LA(1.53, 243)) to fit S 2p, C 1s, Si 2p, and O 1s. S 2p was fit with a doublet peak with a spin-orbit splitting of 1.16 eV.

Temperature-programmed desorption (TPD) measurements were conducted using a Micromeritics Autochem 2920 II equipped with a thermal conductivity detector (TCD). Ammonia (NH₃) was employed as the probe molecule to analyze the acid sites of the samples. Approximately 0.1 g of material was used for each measurement, with the exact mass recorded for each sample. A bed thermocouple monitored the sample temperature throughout the process. Calibration was performed using multiple pulses of 5% NH₃/He through a 507 μ L sample loop. For sample preparation, helium (He) pre-treatment was carried out at a flow rate of 50 mL min⁻¹ at 200°C for 1 hour, with a ramp rate of 10°C min⁻¹, followed by cooling under a continuous He flow. The samples were then saturated with 5% NH₃/He at a flow rate of 30 mL min⁻¹ for 30 minutes at 50°C. Excess NH₃ was removed by purging with He at a flow rate of 30 mL min⁻¹ for 30 minutes. The TPD measurements were subsequently performed under a He flow of 30 mL min⁻¹, heating the sample from 50°C to 700°C at a ramp rate of 10°C min⁻¹, with the final temperature maintained for 1 hour.

Thermogravimetric analysis (TGA) and difference thermal gravimetry (DTG) were performed using a Netzsch TG 209 F1 Libra instrument. The analyses involved monitoring the variations in mass of the monoliths as the temperature was increased. The temperature range was from 30 °C to 800 °C, with a heating rate of 20 °C/min under nitrogen. A Vertex 70 Fourier Transform Infrared (FTIR) spectrometer was employed to analyse the functional groups. The mass ratios of carbon, hydrogen, and sulphur in the material were determined using a CHNS elemental analyser (Elementar Vario Micro cube). The determination of acid density was estimated through NaOH titration.^{2,3} Samples weighing at least 50 mg were soaked in a 50 ml solution of 2 mol/L NaCl for 24 hours under stirring, facilitating the exchange of

protons within the material with Na⁺ ions. The addition of phenolphthalein served as indicator. Subsequently, the acid content was quantified via titration using NaOH solution (5 mmol/L).

Esterification of oleic acid and methanol

The esterification of oleic acid was carried out in autoclaves, followed by placement in an oven at the designated temperature. A mixture comprising 3.17 ml of oleic acid and 4.05 ml of methanol was thoroughly blended prior to the addition of various masses of fabricated catalysts. Catalyst loadings of 1 wt%, 5 wt%, and 10 wt% relative to oleic acid were investigated. To explore the influence of reaction temperature, esterification reactions were conducted at 90 °C, 120 °C, and 150 °C respectively. The resulting products from esterification were processed at 50 °C for 5 hours using a rotary evaporator (Buchi B-480), aimed at removing water and residual methanol. The initial and final acid values were assessed through KOH titration, following procedures outlined in existing literature.^{4,5} Titration was performed using 0.2 mol/L KOH solution, with phenolphthalein solution employed as indicator. The acid value was calculated using following equation:

$$X(AV) = \frac{(V - V_0) \times c \times N(KOH)}{m}$$

where $X(AV)$ (mg/g) represents the acid value, V and V_0 (ml) denote the initial and final volumes of KOH, c (mol/L) is the concentration of KOH, $N(KOH)$ (g/mol) represents the molecular weight of KOH, and m (g) indicates the mass of evaporated esterification production.

The conversion of oleic acid was assessed based on the alterations in acid value, and computed using the following equation:

$$Conversion (\%) = \frac{X(AV1) - X(AV2)}{X(AV1)}$$

where $X(AV1)$ represents the initial acid value of oleic acid, while $X(AV2)$ denotes the acid value of final evaporated esterification production.

For the kinetic study, the conversion data were analysed using a pseudo-first order rate equation to determine the rate constant ' k '.⁶ Turnover frequency (TOF, h⁻¹) is calculated using ' k ' value by the following equation:

$$TOF = \frac{k \times C}{Acid\ density \times Mass}$$

where TOF (h^{-1}) represents the turnover number of a single active site per unit time, C (mmol) denoted the initial mole of oleic acid, $acid\ density$ (mmol/g) is obtained by NaOH titration, $mass$ (g) represents the amount of catalyst used.

In this study, TOF was calculated based on the oleic acid conversion observed during the first hour of the reaction. The reaction condition was: mole ratio of oleic acid and methanol 1:10, reaction temperature $120^{\circ}C$. The TOF values for different catalyst under this reaction condition are included in Table 1.

The slightly higher TOF observed for H-0.2-SO₃-0-Z compared to H-0.2-SO₃-0.5-Z at the beginning of the reaction can be attributed to the greater accessibility of acid sites. In the case of H-0.2-SO₃-0-Z, the acid sites are primarily located on the surface or within macropores, allowing reactants to reach them more easily. Conversely, for H-0.2-SO₃-0.5-Z, a portion of the acid sites are situated within mesopores or micropores, resulting in a slightly lower initial conversion rate. However, over time, the overall catalytic efficiency of H-0.2-SO₃-0.5-Z surpasses that of H-0.2-SO₃-0-Z, as its hierarchical structure facilitates improved mass transfer and reduces diffusion limitations.

The slightly higher TOF observed for H-0.2-SO₃-0.8-Z compared to H-0.6-SO₃-0.5-Z and H-2.5-SO₃-0.5-Z can be attributed to the fact that a significant number of acid sites in H-0.6-SO₃-0.5-Z and H-2.5-SO₃-0.5-Z are densely packed within the micropores. This crowding effect leads to reduced accessibility at the early stage of the reaction, rendering some acid sites inactive or less effective, which in turn lowers the efficiency per active site at the short reaction time.

Table S1. The surface areas and acid density of non-sulfonated monolith and silica

Catalyst	^a S _{BET} (m ² /g)	^b S _{micro-BET} (m ² /g)	^b S _{meso-BET} (m ² /g)	^c -SO ₃ density (mmol/g)	^d Total acid density (mmol/g)
0-Z	280	191.6	88.4	0	0.47
0.5-Z	655.9	221.2	44.7	0	0.46
0.8-Z	719.3	255.8	463.5	0	0.49
H-0.5-Z	543.4	80.6	462.8	0	0.43
SiO ₂ (0.5M CTAB)	1187	12	1175	0	0.08

a: BET method applied to the N₂ isothermal (p/p₀ 0.05-0.3).

b: Surface area of micropores and mesopores, t-plot method applied to the N₂ isothermal.

c: Based on elemental analysis.

d: Based on NaOH titration.

Table S2. Quantification of acid properties calculated from NH₃-TPD analysis with normalisation by mass. Peak temperature is the peak maximum for each sample.

Catalyst	NH ₃ adsorbed (mmol g ⁻¹)	Peak Temperature (°C)
ZSM-5 particle	4.2	123
SO ₃ -ZSM-5 particle	5.0	338
0.5-Z	4.0	113
H-0.6-SO ₃ -0.5-Z	7.5	392

Table S3. A comparative analysis of the catalytic activity of zeolite catalysts in the esterification reaction of oleic acid with methanol.

Catalyst	Temperature (°C)	^a Catalyst loading (wt%)	Molar ratio	Time(h)	Conversion (%)	Reference
Zr-H-ZSM-22	70	11	1:45	8	15	[7]
Zr-H-ZSM-22@SiO ₂	70	11	1:10	8	22	[7]
TPA/MCM-22	60	10	1:12	4	61	[8]
SO ₃ -HM-ZSM-5-3	88	5	1:18	10	100	[9]
0.3HPW/OMS-SO ₃ H-5	120	1.12	1:30	10	90	[10]
Sulfated ZSM-5 nano catalyst	190	5	1:20	8	97	[11]
SO ₃ -ZSM-5 particle	120	5	1:10	5	81	Present work
H-0.6-SO ₃ -0.5-Z	120	5	1:10	3	91	Present work

a: Catalyst loading of 5 wt% compared to acetic acid.

All catalysts listed in the table are in particulate form, with the exception of H-0.6-SO₃-0.5-Z, which is in monolithic form.

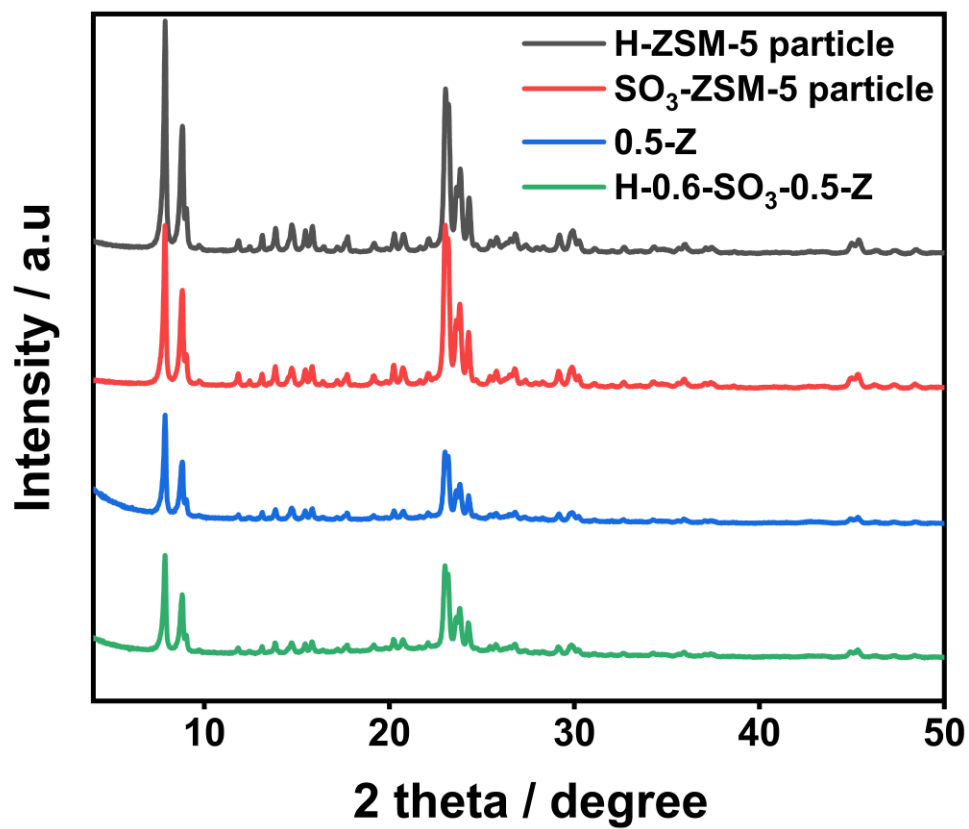


Figure S1. XRD patterns of zeolite particles and zeolite monoliths.

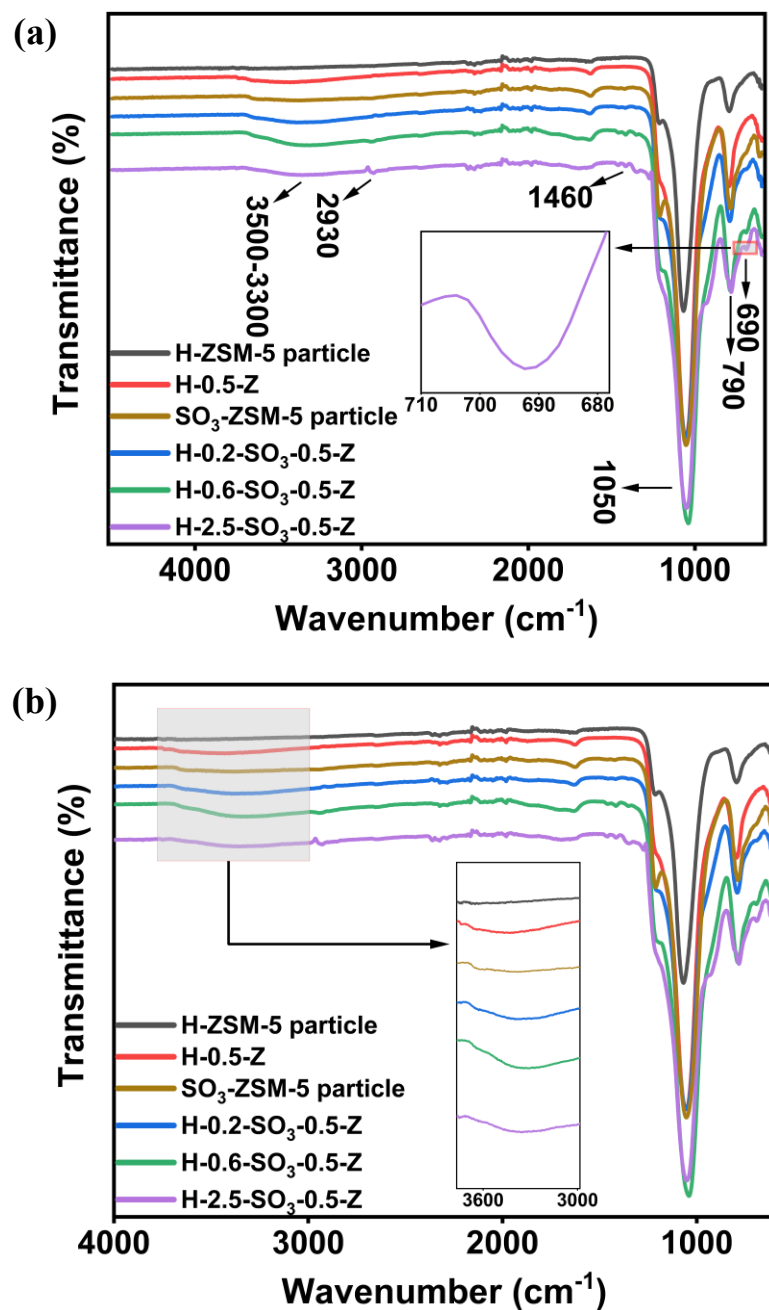


Figure S2. (a) FTIR spectra of zeolite particles and zeolite monoliths. (b) The region for the -OH peaks in the FTIR spectra is expanded to show increasing intensity after sulfonation.

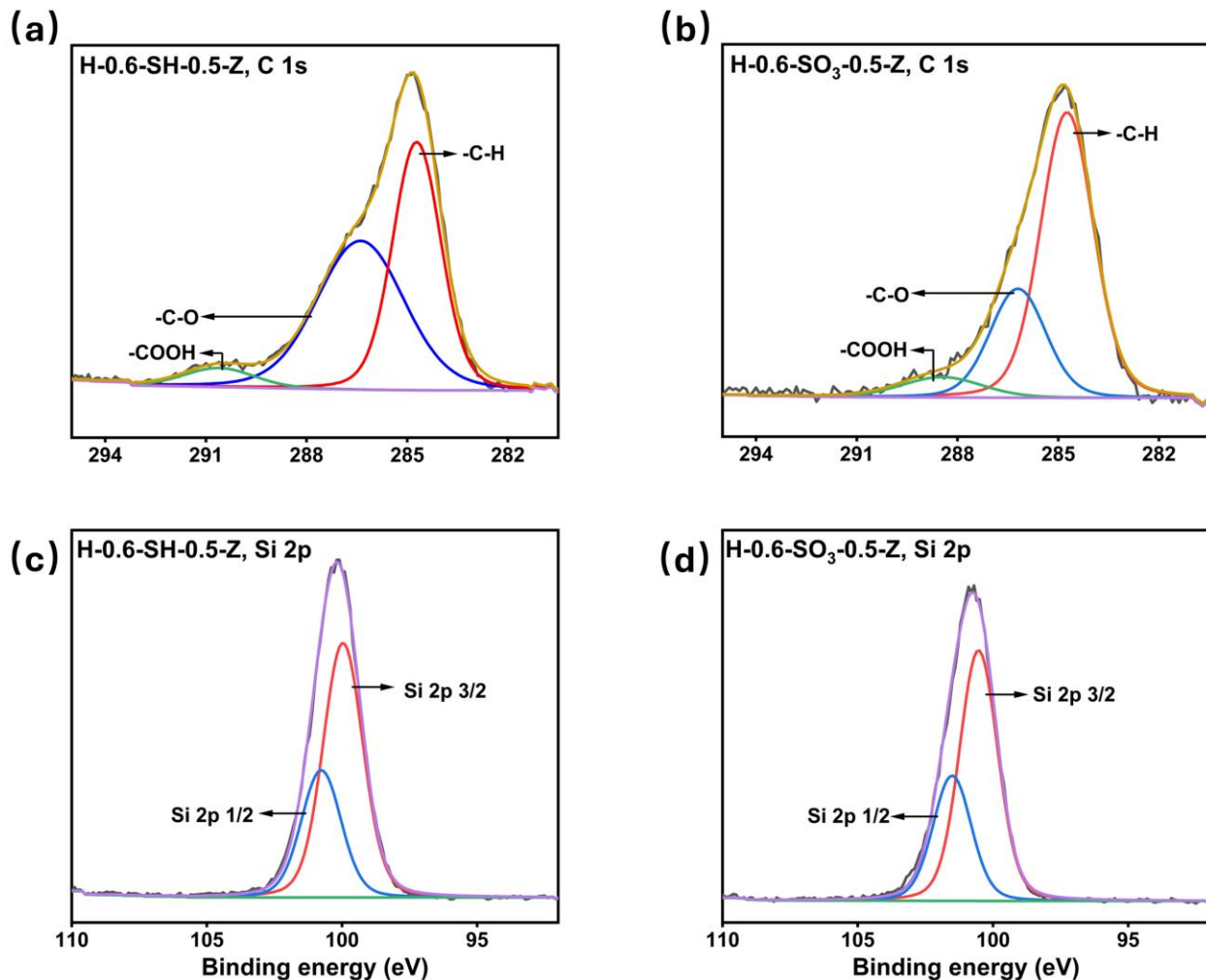


Figure S3. XPS spectra of C 1s and Si 2p for the zeolite monolith H-0.6-SH-0.5-Z and H-0.6-SO₃-0.5-Z. (a) C 1s spectrum for H-0.6-SH-0.5-Z. (b) C 1s spectrum for H-0.6-SO₃-0.5-Z (after oxidizing the monolith H-0.6-SH-0.5-Z to generate -SO₃H groups). (c) Si 2p spectrum for H-0.6-SH-0.5-Z. (d) Si 2p spectrum for H-0.6-SO₃-0.5-Z (after oxidizing the monolith H-0.6-SH-0.5-Z to generate -SO₃H groups).

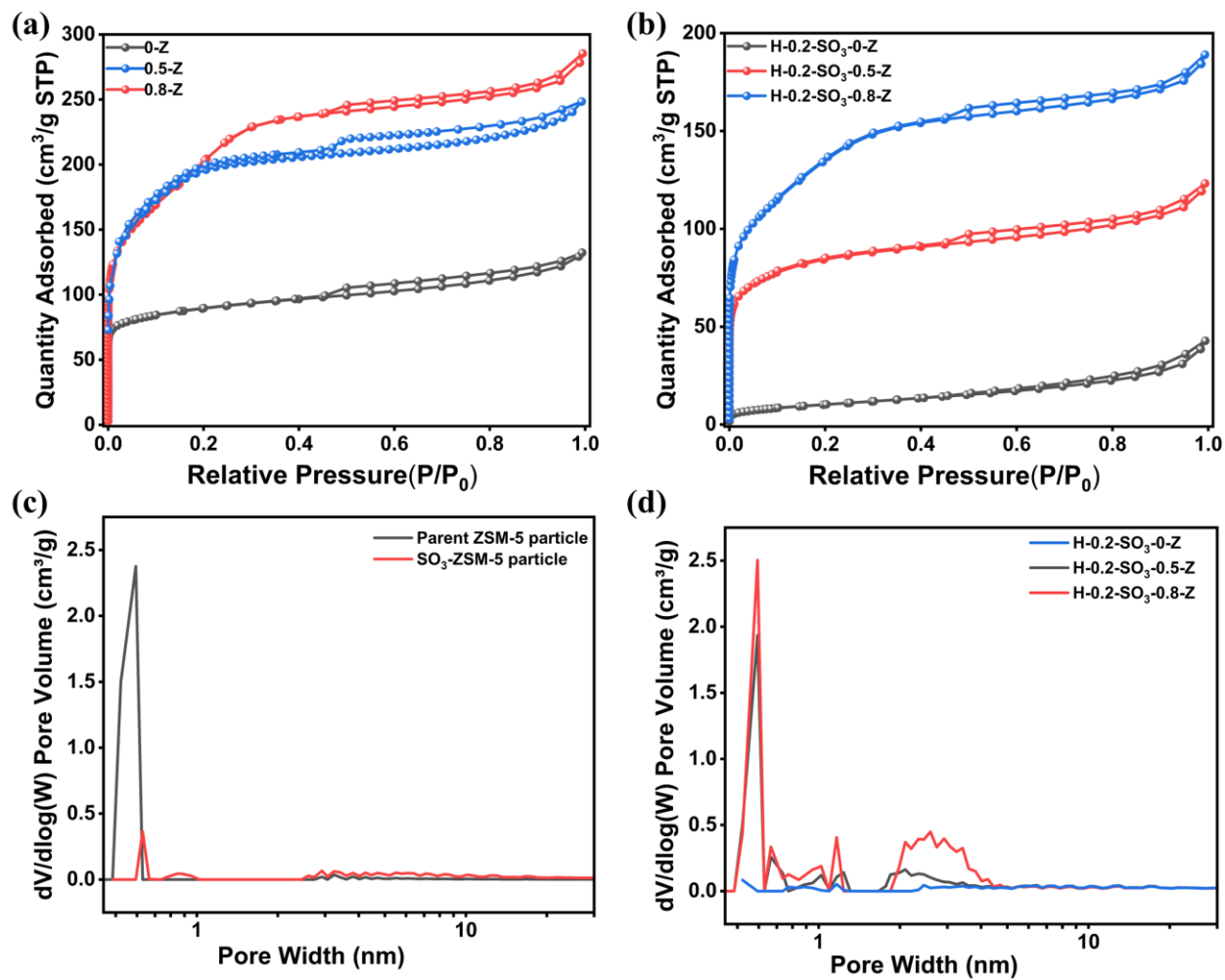


Figure S4. N₂ adsorption-desorption isotherms for zeolite monoliths (a, b) and pores distribution for zeolite particles (as comparison, c) and zeolite monoliths (d).

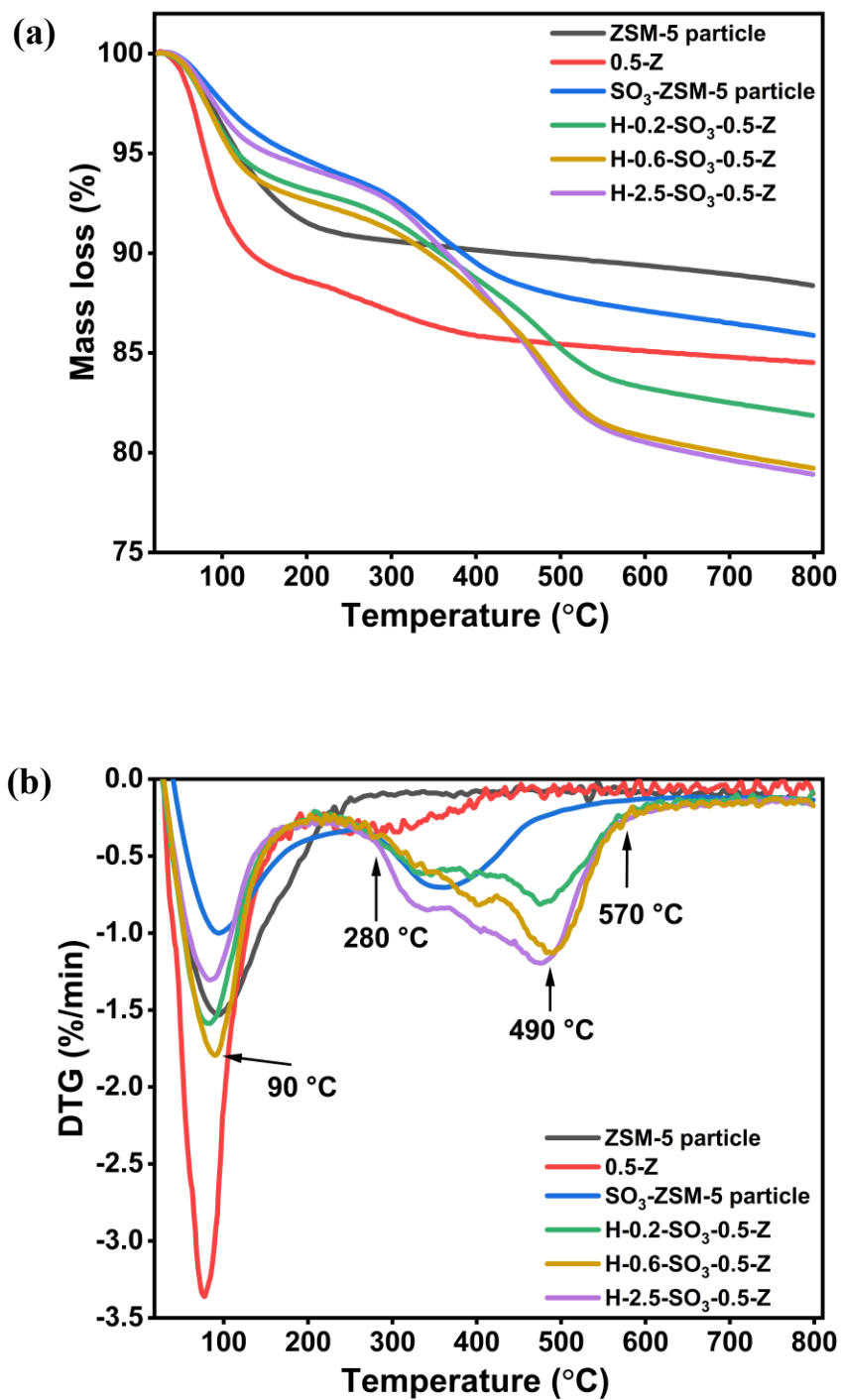


Figure S5. (a) Thermogravimetry analysis (TGA) profiles and (b) differential thermal analysis (DTG) profiles for zeolite particles and zeolite monoliths.

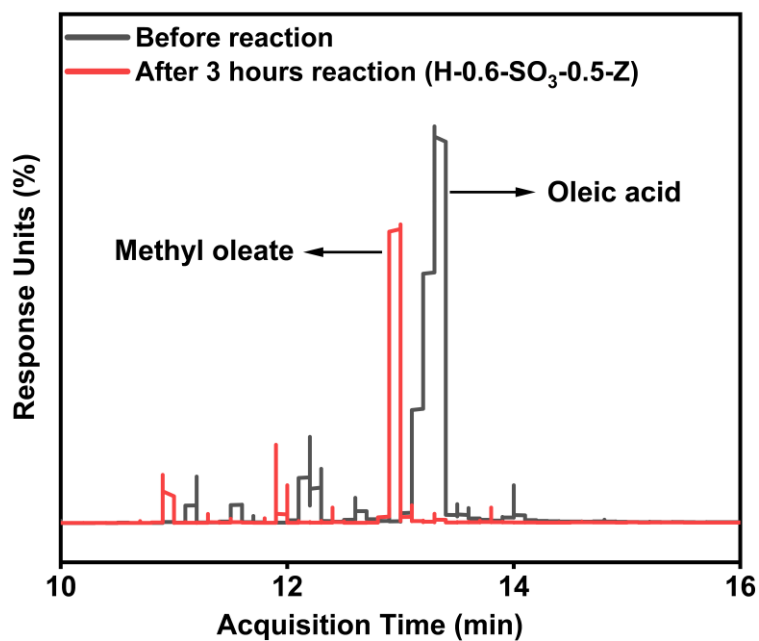


Figure S6. Gas chromatography (GC) spectra of reactants and products before and after the reaction (Catalyst: H-0.6-SO₃-0.5-Z, reaction condition: 120°C, 3h, catalyst loading: 5 wt%). The oleic acid (Sigma-Aldrich) used in this study has a content of oleic acid at 65%-88%. From the GC spectra, oleic acid was converted to methyl oleate. Other small peaks in the graph are other acids and their ester after the reaction.

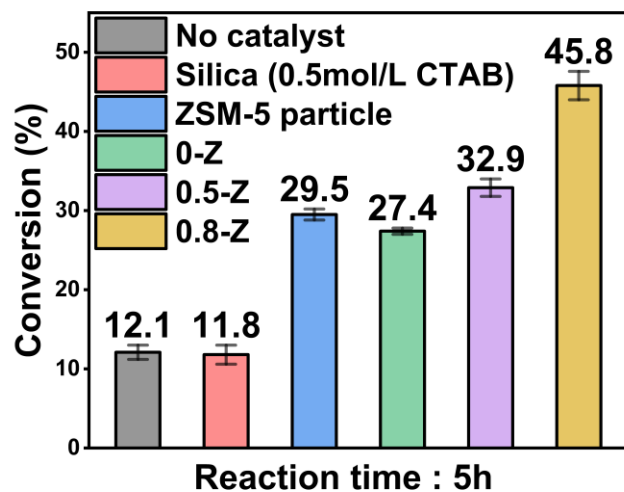


Figure S7. The conversion of oleic acid in the esterification reaction of oleic acid with methanol using non-sulfonated zeolite particles or monoliths as the catalyst. (Reaction condition: 120 °C, catalyst loading: 5 wt%, reaction time: 4h).

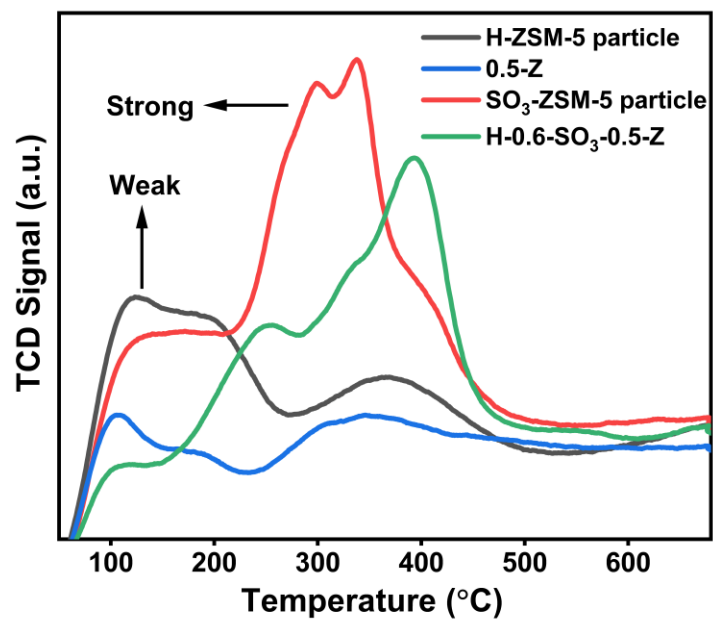


Figure S8. Temperature-Programmed Desorption of Ammonia profile zeolite particles and zeolite monoliths.

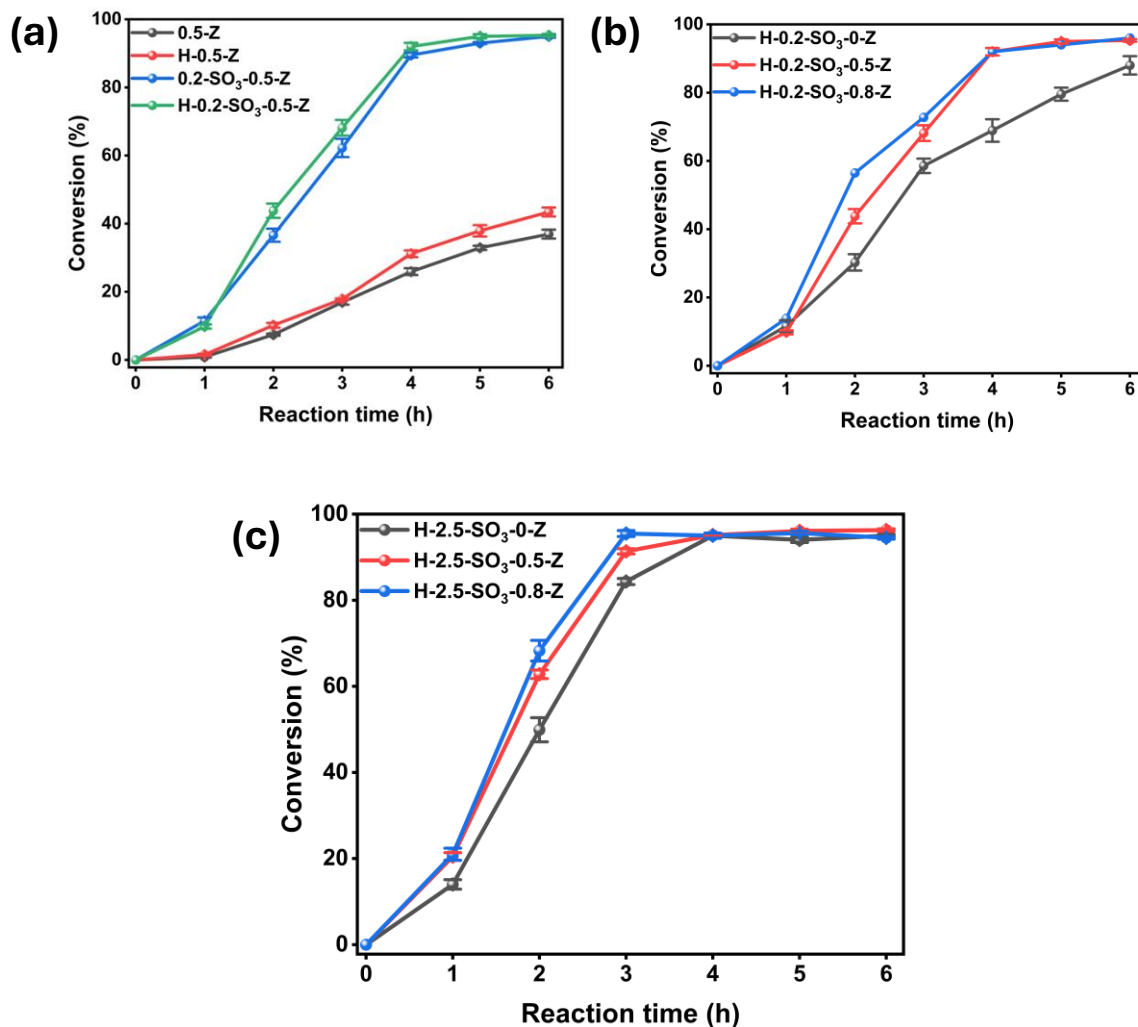


Figure S9. The conversion of oleic acid in the esterification reaction with methanol under different reaction conditions. (a) the effect of HNO₃ treatment during catalyst preparation. (b) the effect of CTAB concentrations (0 M, 0.5 M, 0.8 M) for the monoliths treated with 0.2 g/g of 3-MPTMS. (c) the effect of CTAB concentrations (0 M, 0.5 M, 0.8 M) for the monoliths treated with 2.5 g/g of 3-MPTMS. Standard reaction condition: Temperature 120 °C, catalyst loading: 5 wt% (relative to the oleic acid mass), ratio of methanol to oleic acid: 10:1.

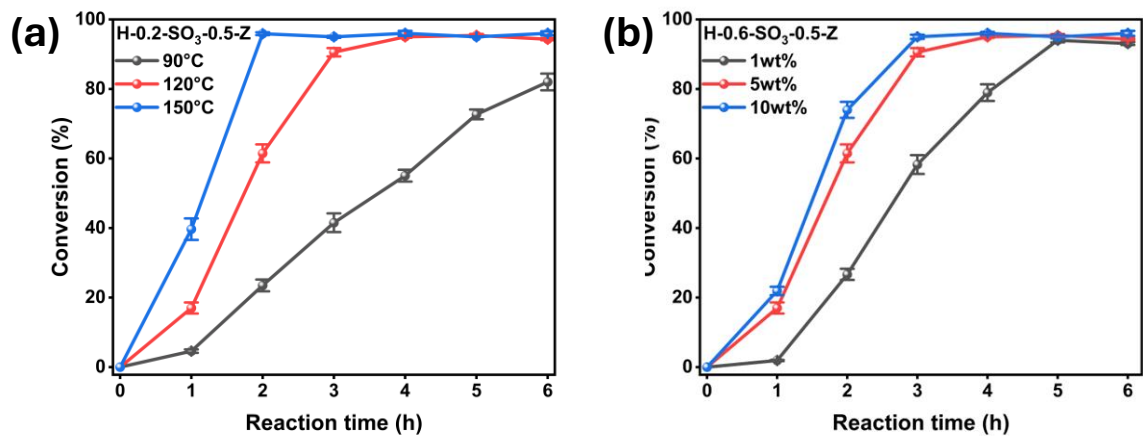


Figure S10. The effect of reaction temperature and catalyst loading on the conversion of oleic acid in the esterification reaction with methanol. (a) The effect of reaction temperature for the catalyst H-0.2-SO₃-0.5-Z. (b) The effect of catalyst loading for the catalyst H-0.6-SO₃-0.5-Z. Standard reaction condition: Temperature 120 °C, catalyst loading: 5 wt% (relative to the oleic acid mass), ratio of methanol to oleic acid: 10:1.

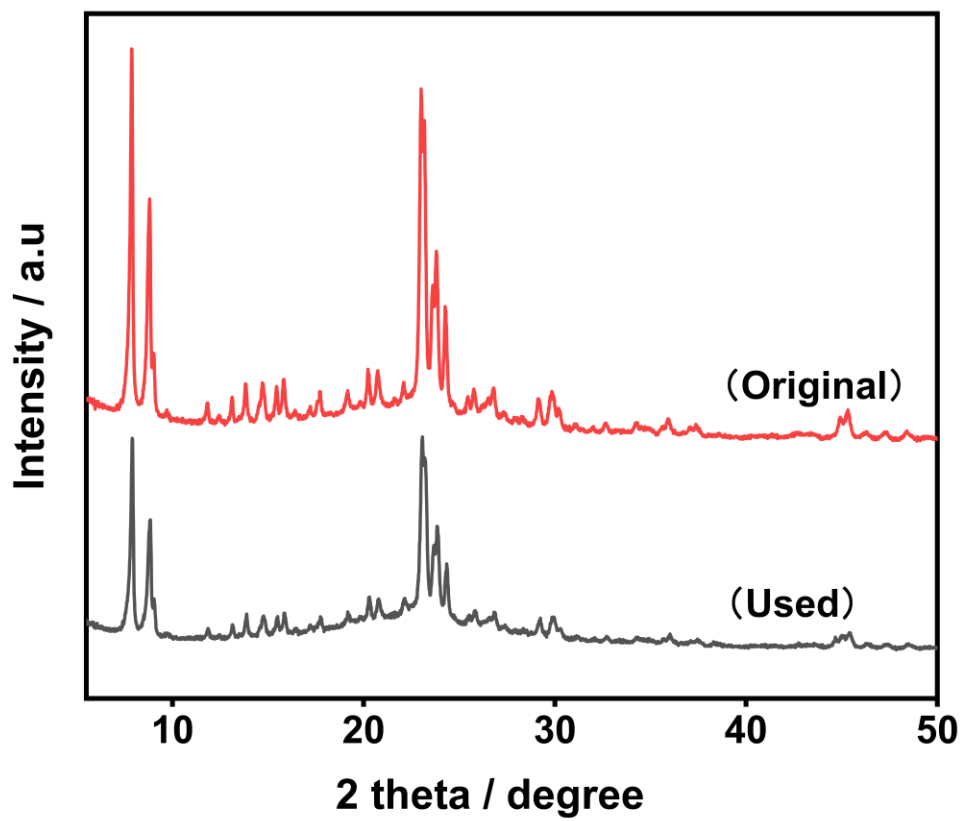


Figure S11. PXRD pattern of original and used sulfonated zeolite monolith H-0.2-SO₃-0.5-Z (After 5 cycles).

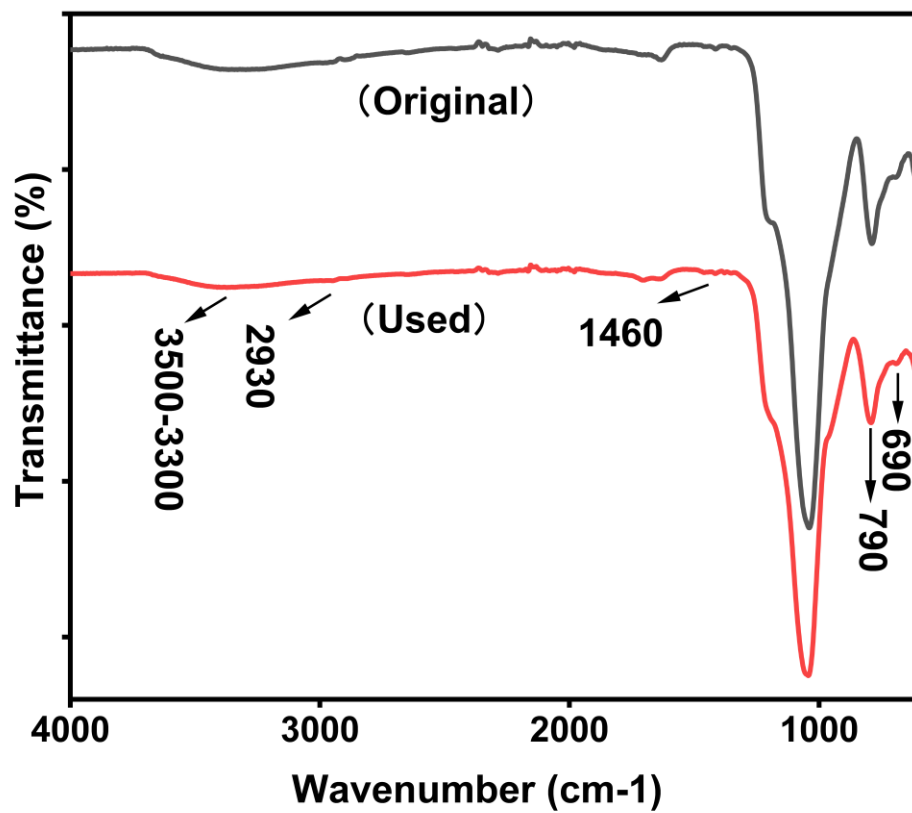


Figure S12. FTIR spectra of original and used sulfonated zeolite monolith H-0.2-SO₃-0.5-Z (After 5 cycles).

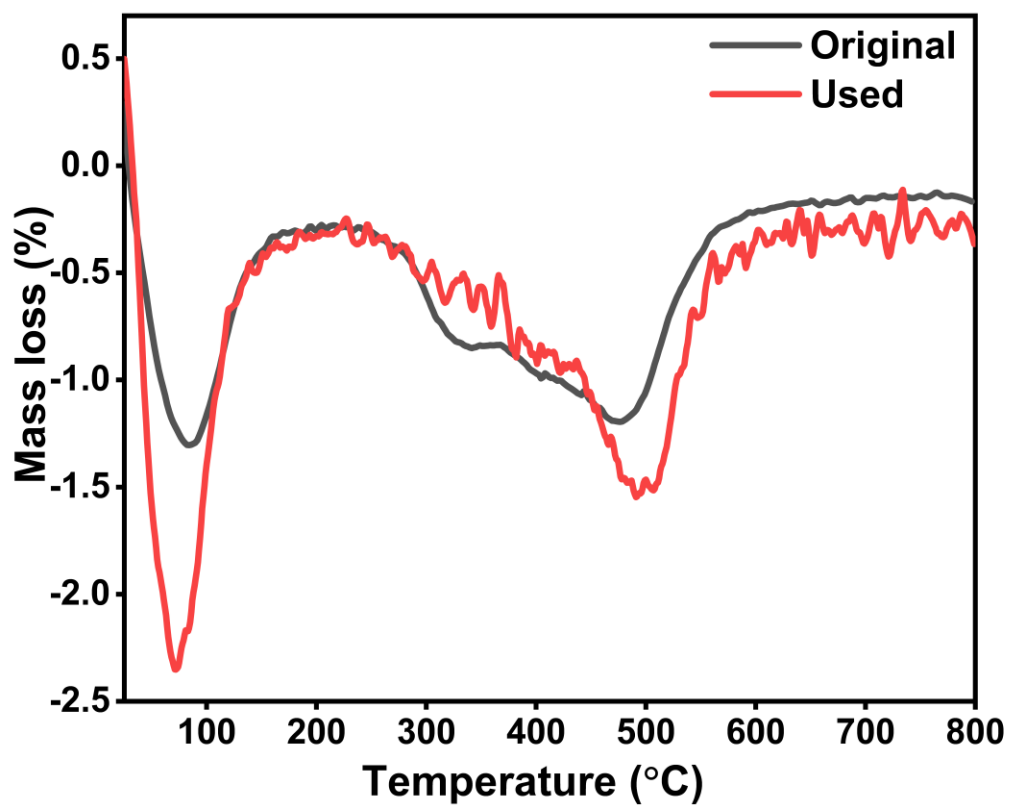


Figure S13. Differential thermal analysis of original and used sulfonated zeolite monolith H-0.2-SO₃-0.5-Z (After 5 cycles).

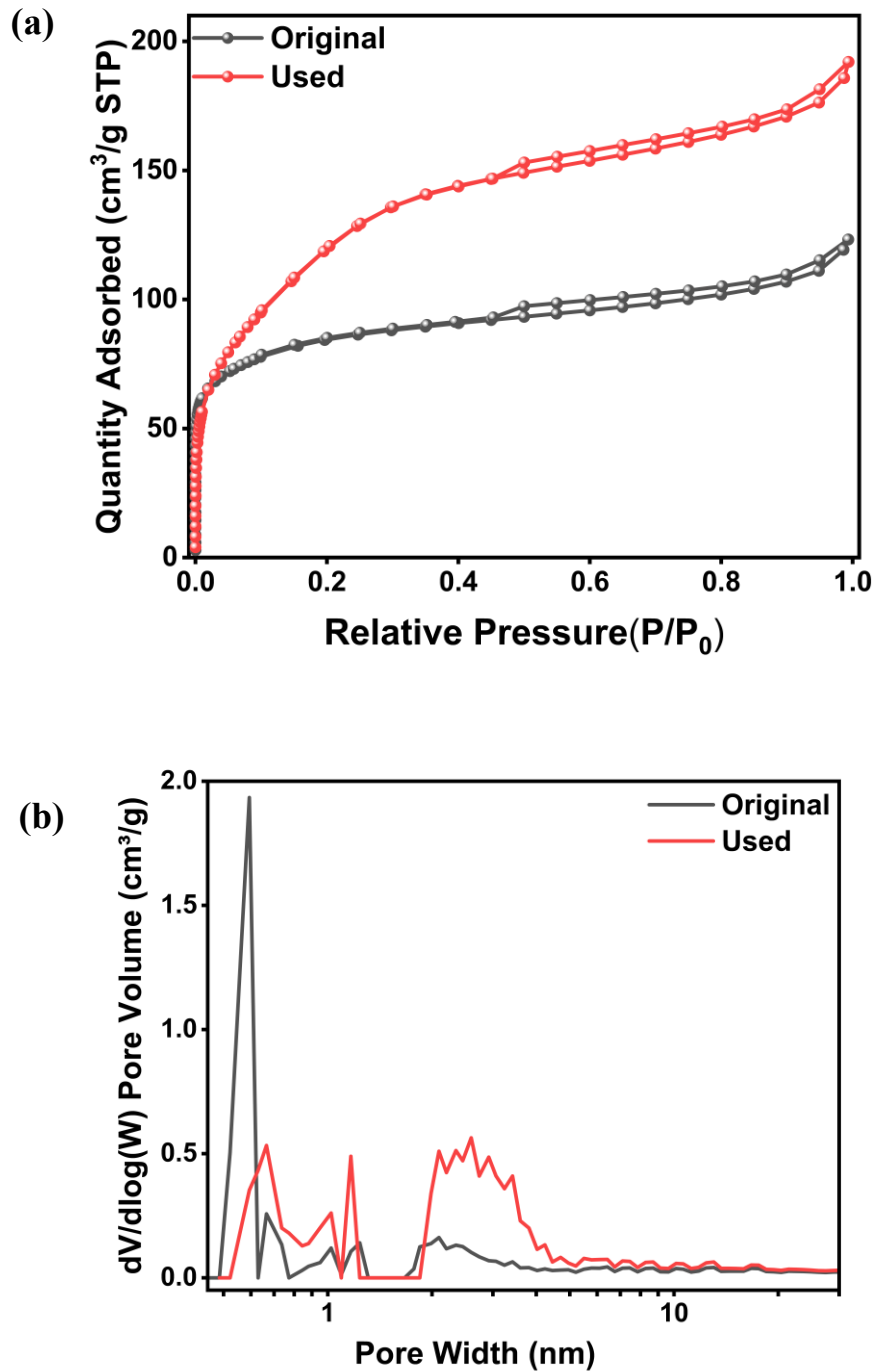


Figure S14. (a) N₂ adsorption-desorption isotherms and (b) pores distribution of original and used sulfonated zeolite monolith H-0.2-SO₃-0.5-Z (After 5 cycles).

Reference

- 1 S. Kadarwati, R. N. Annisa, E. Apriliani, C. Kurniawan and S. B. W. Kusuma, *Trends Sci.*, 2023, 20, 3632.
- 2 W.-Y. Wong, S. Lim, Y.-L. Pang, S.-H. Shuit, W.-H. Chen and K.-T. Lee, *Sci. Total Environ.*, 2020, 727, 138534.
- 3 S. Dechakhumwat, P. Hongmanorom, C. Thunyaratchatanon, S. M. Smith, S. Boonyuen and A. Luengnaruemitchai, *Renew. Energy*, 2020, 148, 897–906.
- 4 A. P. da Luz Corrêa, R. R. C. Bastos, G. N. da Rocha Filho, J. R. Zamian and L. R. V. da Conceição, *RSC Adv.*, 2020, 10, 20245–20256.
- 5 B. Zhang, M. Gao, J. Geng, Y. Cheng, X. Wang, C. Wu, Q. Wang, S. Liu and S. M. Cheung, *Renew. Energy*, 2021, 164, 824–832.
- 6 L. J. Konwar, P. Mäki-Arvela, E. Salminen, N. Kumar, A. J. Thakur, J.-P. Mikkola and D. Deka, *Appl. Catal., B*, 2015, 176, 20–35.
- 7 M. Haghghi and M. Fereidooni, *Int. J. Chem. Eng.*, 2021, 2021, 5321383.
- 8 Pang, G. Yang, L. Li and J. Yu, *Chem. Res. Chin. Univ.*, 2021, 37, 1072–1078.
- 9 N. M. Marzouk, A. O. A. El Naga, S. A. Younis, S. A. Shaban, A. M. El Torgoman and F. Y. El Kady, *J. Environ. Chem. Eng.*, 2021, 9, 105035.
- 10 Z. Yu, X. Chen, Y. Zhang, H. Tu, P. Pan, S. Li, Y. Han, M. Piao, J. Hu and F. Shi, *Chem. Eng. J.*, 2022, 430, 133059.
- 11 S. Mohebbi, M. Rostamizadeh and D. Kahforoushan, *Microporous Mesoporous Mater.*, 2020, 294, 109845.